

10 **Abstract**

11 Sugar beet pulp (SBP) is the major by-product in sugar industry. To make profit out of this
12 undervalued residue, the FASTSUGARS process was proposed as a solution, combining
13 the advantages of supercritical water as hydrolysis medium with very short reaction times
14 in the so-called ultrafast reactors. Operating at 390 °C, 25 MPa and reaction times between
15 0.11 and 1.15 s it was possible to convert SBP into sugars and to obtain a lignin-like solid
16 fraction. The highest yields of C-6 and C-5 sugars (61 and 71 % w/w, respectively) were
17 obtained at 0.11 s with the lowest yield of degradation products. The solid product obtained
18 at 0.14 s was thoroughly analyzed by acid hydrolysis, TGA and FTIR analysis to prove its
19 enhanced thermal properties and aromaticity. The FASTSUGARS process demonstrated
20 being a versatile and promising technology to be integrated in the future biorefineries.

21 **Highlights**

- 22 • FASTSUGARS is a key step towards future sustainable biorefineries
- 23 • Sugars were selectively recovered from sugar beet pulp using SCW as reaction medium
- 24 • Ultrafast reactors allowed accurate control of reaction times in the range of milliseconds
- 25 • The solid product after hydrolysis was mainly composed of an acid-insoluble fraction
- 26 • Thorough characterization of the solid confirmed its lignin-like nature

27 **Keywords**

28 Biorefinery • Continuous process • Glycolaldehyde • Lignin • Supercritical fluids

29 **Abbreviations**

- | | | |
|----|------------|-----------------------------------|
| 30 | 5-HMF | 5-hydroxymethylfurfural |
| 31 | AIF | Acid-insoluble fraction |
| 32 | C-5 sugars | Sugars derived from hemicellulose |
| 33 | C-6 sugars | Sugars derived from cellulose |

34	DLS	Dynamic Light Scattering
35	DTG	Derivative thermogravimetric
36	FTIR	Fourier Transformed Infrared
37	HPLC	High Performance Liquid Chromatography
38	RAC	Retro-aldol condensation products
39	SL	Soluble lignin
40	TGA	Thermogravimetric analysis
41	TOC	Total organic carbon
42	SBP	Sugar beet pulp
43	SCW	Supercritical water

44 **1. Introduction**

45 In the recent years, many studies have focused on the requirements of the future industries
 46 to meet the European Union climate and energy targets for the year 2020. The foundation
 47 of the chemical industry is the conversion of raw materials into fuels, chemicals, materials
 48 and energy. From the past century, fossil resources have been the primary feedstock for
 49 chemical industries (Esposito & Antonietti, 2015). However, the global economy tends to
 50 shift the chemical industry away from petroleum towards renewable raw materials and
 51 sustainable processes in the so-called biorefineries (Apprich et al., 2014; Cocero et al.,
 52 2017).

53 The success of a biorefineries eventually depends on the extent of integration that can be
 54 achieved (*Star-COLIBRI*, 2011) (Okajima & Sako, 2014) (Okajima & Sako, 2014)
 55 (Okajima & Sako, 2014) (Okajima & Sako, 2014). Supercritical fluids are a promising
 56 alternative to integrate the depolymerization, reaction and separation processes (Cantero et
 57 al., 2015a). In fact, using supercritical water (SCW, meaning water above its critical point:
 58 374 °C and 22 MPa) as reaction or extraction medium for biomass has several advantages

59 over other processes: first obvious reason would be its suitability as solvent, being an
60 environmentally friendly and nontoxic medium for chemical reactions (Kumar et al., 2010).
61 Moreover, water itself is one of the constituent of biomass so that, using water as solvent
62 would make unnecessary to previously dry biomass, implying an important energy saving
63 (Peterson et al., 2008). Finally, physical properties of water can be finely tuned by varying
64 temperature and pressure at around its critical point. That would allow fractionation of
65 biomass, since just by changing the reaction conditions it is possible to extract and/or
66 depolymerize the different fractions of biomass. Particularly, operating under SCW
67 conditions, mass transfer resistances are substantially reduced giving as a result faster
68 reaction rates (Peterson et al., 2008). Indeed, certain biomass fraction reactions that
69 occurs in the range of milliseconds. Then, changing the reaction time from minutes to
70 milliseconds, allows the reactor volume being reduced from m^3 to cm^3 and therefore
71 implies an important equipment cost reduction (Cantero et al., 2015a). That drastic reaction
72 time reduction is a strong step forward the process intensification of biomass usage. The
73 intensification of biomass use as feedstock is of utmost importance in the development of
74 compact and efficient facilities, consuming local available biomass and providing local
75 needs. Moreover, SCW technology could be integrated with power generation by gas
76 turbines, injecting the steam produced in the hydrolysis process to the combustor (Cantero
77 et al., 2015c). That integration results in very low extra energy consumption when coupling
78 SCW hydrolysis and heat and power generation.

79 There is more than one parameter to evaluate when choosing a feedstock to develop the
80 biorefinery concept. When pursuing industrial sugars, like glucose or xylose, plus lignin; it
81 becomes very important to consider as a feedstock a cheap and highly available feedstock.
82 In that sense, the agro-industrial byproducts are considered promising resources for the
83 production of sugars and lignin (Concha Olmos & Zúñiga Hansen, 2012). This is the case
84 of sugar beet pulp (SBP), which is the major by-product in beet sugar industry. It is
85 composed of 20 – 25 % cellulose, 22 – 30 % hemicellulose, 24 – 32 % pectin, 10 – 15 %
86 protein and 1 – 3% insoluble lignin on a dry basis (Zheng et al., 2013; Zieminski et al.,
87 2014). Due to its low insoluble lignin and high carbohydrates content, sugar beet pulp is an
88 interesting candidate for both sugars recovery and platform chemical production in the
89 future biorefineries (Kühnel et al., 2011). In some cases, the sugar plants from beet possess

90 an internal heat and power generation systems by gas turbines. This fact presents an
91 opportunity to link SCW hydrolysis of SBP with heat and power production by gas
92 turbines.

93 During the past years, several authors studied the fractionation of SBP to obtain ferulic acid
94 (Bonnin et al., 2002; Saulnier & Thibault, 1999), arabinoxylans and/or pectic substances
95 (Leijdekkers et al., 2013; Spagnuolo et al., 2000). To do so, enzymatic hydrolysis was the
96 preferred method to release those components. However, the high dosage of enzymes
97 and/or chemicals required to release sugars is still a concern in the operating cost side,
98 presenting a significant barrier to commercialization (Merino & Cherry, 2007). Moreover,
99 for SBP being a complex mixture of cellulose, hemicellulose and pectin, the efficient
100 enzymatic conversion of the whole crop is still a problem to be solved (Kühnel et al.,
101 2011). Dilute acid pretreatments are usually presented as a solution (Zheng et al., 2013) but
102 they have important drawbacks such as equipment corrosion, poor catalyst recyclability and
103 sugars degradation (Prado et al., 2016). To overcome these limitations, SCW technology
104 has demonstrated being a promising alternative to transform biomass into sugars with
105 several advantages over conventional process. It produces less sugars degradation
106 compared to acid/alkali methods and it allows equipment and time reduction compared to
107 enzymatic routes (Prado et al., 2016). In the recent years near-critical water hydrolysis of
108 agricultural and food industry residues has been intensively studied, but SCW hydrolysis
109 studies are still limited (Cantero et al., 2015b; Jeong et al., 2017; Zhao et al., 2012).

110 Considering the complexity of the matrix interactions and the diversity of their
111 compositions, each biomass represents a technological challenge that should be studied
112 separately (Prado et al., 2016). In this work, sugar beet pulp was hydrolyzed for the first
113 time in supercritical water for sugars recovery in the so-called FASTSUGARS process. The
114 reaction temperature for this study was dropped from previous studies at 400 °C to 390 °C
115 to evaluate the ability of the system to still produce high selective hydrolysis while cutting
116 the energy demand. To do so, the hydrolysis was carried out in a continuous flow type
117 reactor setup, called as ultrafast reactor from now on. Since the sugar industry from beet
118 shows a perfect example for the integration of sugars and lignin production from residual
119 biomass with the heat and power production systems by gas turbines, the aim of this work

120 was to optimize the ultrafast SCW hydrolysis to convert SBP into sugars, platform
121 chemicals and lignin-like solid products.

122 **2. Materials and Methods**

123 **2.1. Materials**

124 A local sugar industry (ACOR, Spain) provided the SBP used in the experiments. It was
125 milled to obtain an average particle size of 60 μm . Deionized water was used as the
126 reaction medium to run the experiments. The High Performance Liquid Chromatography
127 (HPLC) standards were purchased from Sigma-Aldrich, being: cellobiose, galacturonic
128 acid, glucose, xylose, fructose, arabinose, glyceraldehyde, pyruvaldehyde, glycolaldehyde,
129 lactic, formic and acetic acids and 5-hydroxymethylfurfural (5-HMF). Milli-Q water and
130 sulfuric acid were used as the mobile phase in the HPLC analysis. For the determination of
131 carbohydrates and lignin, sulfuric acid and calcium carbonate supplied by Sigma were
132 employed as reagents. The pectin identification assay kit from Megazyme was used to
133 determine the pectin fraction in biomass. For this purpose, Trizma base and sodium
134 hydroxide pellets were purchased from Sigma and hydrochloric acid solution 5 M was
135 purchased from Fluka. For Kjeldahl determination of protein content, Kjeldahl catalyst
136 (Cu) (0.3% $\text{CuSO}_4 \cdot 5\text{H}_2\text{O}$) tablets were purchased from PanReac.

137 **2.2. Methods**

138 **2.2.1. Chemical characterization of the raw sugar beet pulp**

139 Laboratory Analytical Procedure from the National Renewable Energy Laboratory (NREL)
140 was used to determine the structural carbohydrates (namely, cellulose and hemicellulose)
141 and lignin content in the biomass (Sluiter et al., 2010). This same protocol was described in
142 a previous work in which wheat bran was characterized (Cantero et al., 2015b). Using this
143 procedure, it was possible to quantify the extractives, cellulose, hemicellulose, ash,
144 insoluble and soluble lignin in sugar beet pulp. The particle size of the starting material was
145 measured using a Dynamic Light Scattering (DLS) Mastersizer 2000. The mean particle
146 size was 60 μm . Total Kjeldahl nitrogen was determined according to APHA Sandards
147 Methods and then total proteins were calculated as Kjeldahl N \times 6.25 (Lynch et al., 2008),
148 calculated using Eq. S1 shown in Supporting material.

149 The pectin identification assay kit from Megazyme was employed to determine the pectin
150 fraction in SBP. Using this kit, pectin was dissolved in water at pH 12, yielding
151 polygalacturonic acids through the conversion of pectin into pectate. The pectate was
152 incubated with pectate lyase enzyme which broke the polygalacturonic acid, releasing
153 unsaturated oligosaccharides which absorbed at 235 nm (Hansen et al., 2001). As this kit
154 contained pectin from SBP as a standard, the pectin content was determined considering
155 that the absorbance from the pectin standard equaled to 100 % pectin content and therefore
156 the pectin percentage in raw material was calculated by comparison.

157 **2.2.2. Analysis**

158 The composition of the liquid product was determined by HPLC analysis, using a Shodex
159 SH-1011 column as described in previous works (Cantero et al., 2015b; Martínez et al.,
160 2015). The carbon content in the liquid product was determined by total organic carbon
161 (TOC) analysis with Shimadzu TOC-VCSH equipment.

162 The solid product was separated by centrifugation, dried at 105 °C for 24 h and weighted to
163 determine the suspended solids. Then, its composition was determined following the same
164 NREL procedure used for lignin determination in the raw material (Sluiter et al., 2010).
165 Elemental C-S analyser, using a LECO CS-225 equipment, determined the carbon content
166 of the raw material and remaining solids. The solid fraction was also analyzed by
167 spectroscopy Fourier Transformed Infrared (FTIR) by using a Bruker Tensor 27.
168 Thermogravimetric analysis (TGA) was carried out in a TGA/SDTA RSI analyzer of
169 Mettler Toledo.

170 **2.2.3. Experimental setup**

171 The experiments with SBP were performed in the continuous hydrolysis plant of the so-
172 called FASTSUGARS process. This FASTSUGARS plant was designed and built in a
173 previous work of our research group, which operating procedure was deeply described
174 before (Cantero et al., 2013; Cantero et al., 2015b; Martínez et al., 2015). The reaction
175 section was modified for this work as shown in detail in Fig. S1 (supporting material).

176 Then, the key factor in the FASTSUGARS process was the accurate control of the reaction
177 time, meaning the time that biomass and SCW spent together between the mixing point and
178 the reactor outlet. This was possible due to the unique characteristics of the FASTSUGARS
179 reactor. The reactions were instantaneously stopped by a sudden cooling generated by
180 decompressing the reactor from ~25MPa to ~0.2 MPa. That pressure drop produced an
181 instantaneous cooling effect by massive steam explosion (also known as Joule-Thomson
182 effect). This cooling mechanism uniquely stopped the reactions. The reaction times, ' t_R ' in
183 seconds, were calculated as shown in Eq. 1. The reactor volume, ' V ' in m^3 , was calculated
184 using the dimensions of the reactor. The volumetric flow in the reactor, ' F_v ' in m^3/s , was
185 calculated as a function of the density of the reaction medium at ambient conditions ' ρ_0 '
186 and reaction conditions ' ρ_r ', both in kg/m^3 and considering the fluid as pure water. Using
187 the ratio ' ρ_r/ρ_0 ', it was possible to transform the flow measured at ambient conditions, ' $F_{v,0}$ '
188 in m^3/s , into ' F_v '. Therefore, in order to change the reaction time for the different
189 experiments, either reactor's length, total flow or both were varied.

$$190 \quad t_R = \frac{V}{F_v} = \frac{\pi \cdot L \cdot D^2}{4} \frac{\rho_r}{F_{v,0} \cdot \rho_0} \quad (1)$$

191 **3. Results and discussion**

192 **3.1. Biomass characterization and calculations**

193 The compositional analysis of the raw material is shown in Table 1. The lignin fraction was
194 a result of the sum of both soluble and insoluble lignin fractions, being 4.4% insoluble
195 lignin and 18.4% soluble lignin (measured at 280 nm in a spectrophotometer, using 17.084
196 L/g·cm as extinction coefficient obtained as the average of extinction coefficients from
197 literature (Fukushima & Hatfield, 2004)).

198 The sugar beet pulp was hydrolyzed in supercritical water at 390 ± 5 °C and 25 ± 5 MPa at
199 different reaction times in the FASTSUGAR plant. In Table 2, the main parameters used
200 for carbon balance were presented, which were calculated using the equations shown in the
201 supporting material. The carbon balance in the experiments was around 100%. The results
202 of carbon balance calculations are presented in Table S1 (supporting material), meanwhile
203 HPLC results are shown in Table S2. Then, with all those data specific yields of each

204 compound were calculated and presented in Table S3 and also overall yield, conversion and
205 selectivity to sugars in the liquid effluent as shown in Table S4.

206 **3.2.Liquid product characterization**

207 The main hydrolysis parameters were plotted in Fig. 1 and also presented in Table S4. In
208 Fig. 1 it can be seen that C-6 and C-5 yields showed the same trend, since both decreased as
209 reaction time increased. That was the expected trend for biomass hydrolysis in supercritical
210 water, since the reactions of cellulose and hemicellulose hydrolysis were very fast in SCW
211 and very short reaction times were required to hydrolyze these fractions to sugars. In fact,
212 as reaction time increased, the produced sugars from both cellulose and hemicellulose
213 would be degraded into other products (see schematic reaction pathway at Fig. 2), therefore
214 decreasing the yields of sugars. So, for SBP it was possible to recover up to 71 % w/w of
215 hemicellulose as C-5 sugars and at the same time 61 % w/w of cellulose was recovered as
216 C-6 sugars at 0.11 s reaction time. Although hemicellulose was degraded faster than
217 cellulose, it can be seen that both polymers hydrolysis yielded similarly high sugars
218 recoveries. Reaction kinetics for cellulose were highly increased approaching hemicellulose
219 values and both yield were kept high because of the strict control of the reaction time in the
220 FASTSUGARS process. In previous studies, the hydrolysis of pure cellulose in
221 supercritical water was carried out under similar conditions (400°C, 25 MPa) in the
222 FASTSUGARS plant, allowing to recover up to 98 % w/w of inlet cellulose as C-6 sugar
223 after 0.02 s of reaction time (Cantero et al., 2013). However, when hydrolyzing a real
224 biomass such as wheat bran under same conditions, it was found that higher reaction times
225 were needed to obtain high recoveries of both cellulose and hemicellulose sugars (Cantero
226 et al., 2015b).

227 Comparing SBP to wheat bran results, despite their differences, they showed very similar
228 values for maximum C-6 yield (being 63 % w/w for wheat bran and 61 % w/w for SBP).
229 However, these results were not obtained under same reaction time conditions, since for
230 wheat bran maximum C-6 yield was achieved at 0.22 s meanwhile for SBP just 0.11 s were
231 necessary. A possible reason might be the particle size of each biomass, being 60 µm for
232 SBP and 125 µm for wheat bran. Wheat bran having a higher particle size would need
233 higher reaction time to get same yield than sugar beet pulp. In fact, taking into account the

234 conversion calculated by Eq. S11 and shown in Table S4, it could be seen that under same
235 reaction time conditions (experiments at 0.19 s were performed for both biomass), the
236 conversion for SBP was 99 %, meanwhile for wheat bran it was lower (93 %),
237 corroborating that having a bigger particle size, higher reaction time was required to
238 achieve same conversion and therefore same C-6 yield from cellulose. It was already
239 proved that biomass particle size significantly affected hydrolysis processes, since smaller
240 particles have larger surface area per unit of volume, improving the accessibility to
241 cellulose and hemicellulose fractions (Dasari & Eric Berson).

242 In order to better understand the different reactions simultaneously occurring during SBP
243 hydrolysis in SCW, Fig. 1 represented also the yield of the main components detected by
244 HPLC in the liquid product, also separately shown in Table S3 (supporting material).
245 Moreover, the reaction pathway for both cellulose and hemicellulose hydrolysis in SCW
246 was shown in Fig. 2, where it could be seen that once the monomeric sugars from cellulose
247 (glucose and fructose) and from hemicellulose (xylose and arabinose) were obtained they
248 could yield retro-aldol condensation (RAC) products and/or acids. Then, C-5 and C-6
249 sugars, RAC and acids yields were plotted together in Fig. 1. As it can be seen in the figure,
250 for C-6 sugars the yield remained constant (being around 55 %) when reaction times were
251 between 0.11 and 0.23 s and then suddenly decreased to 10 % at 1.15 s. The conversion
252 achieved for reaction times between 0.11 and 0.23 s was close to 100 % but it only reached
253 100 % at 1.15 s. This fact would suggest that reactions times higher than 0.23 s were
254 needed to get total conversion and therefore complete access to the intricate biomass
255 matrix. Then, as reaction time increased, more severe reaction conditions were achieved
256 and complete conversion was obtained as a result, releasing the most resistant fractions of
257 biomass and making them available for hydrolysis. With a higher reaction time, the
258 hydrolysis of that released cellulose would lead to degradation instead of sugars production,
259 drastically decreasing the C-6 sugars yield. So that, conversion gave an idea of the extent of
260 the hydrolysis reaction. On the other hand, for C-5 sugars, a more pronounced decrease
261 occurred when increasing reaction time. Since hemicellulose is more labile than cellulose, it
262 was more rapidly degraded as reaction time and conversion increased. The behavior of both
263 C-5 and C-6 yields matched the behavior of RAC and acids yields. As reaction time
264 increased, the sugars yields decreased and at the same time the degradation products yields

265 increased, due to the transformation of the sugars into RAC products and/or acids. When
266 looking at Table S3 it can be seen that the overall degradation yield (considering RAC
267 products, acids but also 5-HMF) at 0.11 s was 44 %, due to cellulose and hemicellulose
268 degradation, but also from pectin hydrolysis as shown in Fig. 2. Pectin is representing 28%
269 of the feedstock and is a structural heteropolysaccharide which repeating unit is D-
270 galacturonic acid that forms a hydrated gel that “glues” the cell wall components together
271 (Himmel et al., 2007). Pectin also contains neutral sugars as rhamnose, arabinose, mannose,
272 galactose, xylose and even glucose in its chains (Chen et al., 2016). Those free sugars
273 seemed to be already degraded at 0.11 s, yielding glycolaldehyde and residual galacturonic
274 acid from the very beginning. So that, even though the highest sugars yield was achieved,
275 some degradation was already going on at the shortest reaction time mostly due to pectin
276 hydrolysis. Anyway, as the objective in this work was to obtain the highest sugars yield
277 with the lowest degradation, 0.11 s was found to be the optimal reaction time for the
278 production of sugars from SBP through supercritical water hydrolysis in the
279 FASTSUGARS plant. In fact, as a real application for the effluent of this process, the liquid
280 product from SBP hydrolysis in SCW by the FASTSUGARS process produced in parallel
281 to this work was hydrogenated over Ru/MCM-48 to obtain a mixture of hexitols and
282 ethylene glycol (Romero et al., 2016), which is a widely applied feedstock in the plastic and
283 polyester industries. Therefore, it was proved that the liquid effluent obtained via the
284 FASTSUGARS process was a suitable feedstock for the future biorefineries to produce
285 valuable products from biomass that could compete with the petroleum-derived products.

286 The conventional method for sugars’ recovery from SBP consisted on enzymatic
287 hydrolysis, usually with a previous dilute acid pretreatment. The goal of the pretreatment
288 was to solubilize hemicellulose and make residual cellulose more degradable by enzymes
289 (Zheng et al., 2013). The authors of that previous work obtained a liquid rich in C-5 sugars
290 (arabinose recovery was up to 68 % w/w) and the 5-HMF yield was around 10 % w/w after
291 acid pretreatment. Then, after the enzymatic hydrolysis the total reducing sugars yield was
292 around 60 % w/w. For the current work, Table S3 showed the detailed composition of raw
293 SBP in terms of constituent sugars together with the recovery for each individual sugar at
294 different reaction times. It can be seen that maximum glucose recovery was up to 64 % w/w
295 and 74 % w/w of the arabinose was recovered after the FASTSUGARS process. On the

296 other hand, the maximum total sugars yield was 66 % w/w, with a 5-HMF yield of 2 %
297 w/w. So that, when compared to enzymatic hydrolysis, the FASTSUGARS technology
298 allowed improving both cellulose and hemicellulose recovery as sugars in just one efficient
299 step, increasing total sugars yield and reducing fermentation inhibitors at the same time.
300 Another aspect to take into account when comparing SCW technology to conventional
301 enzymatic hydrolysis would be the thermo-economical and environmental analysis. In a
302 previous study, both processes were compared for sugar cane bagasse hydrolysis and it was
303 concluded that SCW technology allowed reducing the total investment of the biorefinery
304 and the water intake (Albarelli et al., 2017). Moreover, several alternatives were proposed
305 to improve the energetic efficiency of the FASTSUGARS process, from the coupling of the
306 ultrafast reactors to commercial combined heat and power (CHP) systems (Cantero et al.,
307 2015c) to the use of a green desuperheater as an alternative to decompression valve
308 (Vaquerizo & Cocero, 2018). So that, the improved yields obtained in the case of SBP and
309 the lower cost associated to SCW technology, proved that FASTSUGARS process is a
310 promising and versatile technology to convert biomass into sugars in a sustainable way.

311 Then, if comparing the current results to the ones obtained from similar technologies
312 involving SCW hydrolysis of agricultural biomass, FASTSUGARS technology also
313 improved existing results. When converting corn stalks under combined supercritical and
314 subcritical conditions in a flow reactor, the maximum recovery of C-6 sugars was 68 %
315 w/w with less than 2 % w/w of C-5 sugars (Zhao et al., 2012). The supercritical reaction in
316 that study was carried at 380 °C with a reaction time of 9 seconds. Comparatively speaking,
317 reducing temperature in that work, slowed down the cellulose hydrolysis rate, which
318 allowed obtaining slightly higher C-6 sugars recovery compared to the current work.
319 However, increasing reaction time resulted in total degradation of hemicellulose, which not
320 occurred in the present study. All in all, operating with the FASTSUGARS plant at 390 °C
321 and 0.11 s it was possible to simultaneously and selectively recover both cellulose and
322 hemicellulose as sugars.

323 **3.3.Solid product characterization**

324 Once the liquid effluent was completely characterized, the solid product composition
325 compared to the raw material composition was shown in Fig. 3. As it was shown in Table

2, the amount of solid obtained after each experiment was almost negligible in terms of mass, but it was important to study the evolution of the hydrolysis process with time regarding the remaining solid composition and also allowed closing the mass balance. Lignin is a complex high molecular weight compound with highly random structure, which makes it difficult to completely liquefy the lignin fraction from biomass (Brunner, 2014). Under the conditions selected for the current work remaining solid was always obtained, so it was not possible to achieve total liquefaction of the initial biomass. That was probably due to the depolymerization and repolymerization reactions that lignin was suffering under supercritical water conditions (Wahyudiono et al., 2008) that produced a solid mostly insoluble in acid. In fact, as it can be seen in Fig. 3, the main fraction found in the solid product was that acid-insoluble fraction (AIF) in all cases. The AIF content in the remaining solid increased when increasing reaction time, meanwhile the hydrolysable fractions, decreased with reaction time. In Fig. 3 it can be seen that the amount of sugars still trapped in the remaining solid at the shortest reaction time was as high as 25 % w/w, suggesting that higher reaction times were needed to fully hydrolyze cellulose and hemicellulose to sugars. Then, when increasing the reaction time above 0.14 s, the sugars content in the remaining solid continuously decreased from 21 % w/w at 0.14 s to 1 % at 1.15 s.

In order to better understand the effect of SCW hydrolysis on the solid product and the nature of its AIF, thermogravimetric analysis (TGA) was performed to a solid sample obtained after supercritical water hydrolysis, being the operating conditions 392 °C, 25 MPa and 0.14 s and also to the raw material. TGA and DTG (derivative thermogravimetric) profiles for both raw material and solid after reaction were presented in Fig. 4. In terms of complex biomass, it is widely accepted that its thermal degradation is divided in three stages: first moisture drying, then a devolatilisation that takes place in the range of 200 – 400 °C which is related to the labile fractions from biomass. This degradation process is then followed by a continuous slight devolatilisation related to lignin (Fisher et al., 2002; Idris et al., 2010). In Fig. 4 it can be seen that the raw material TG curve corroborates the behavior mentioned above, since a first important weight loss was occurring between 200 and 370 °C, corresponding to first hemicellulose and pectin and then cellulose degradations. After that, a continuous plain decreasing curve started at 370 °C to 850 °C that would be

357 related to continuous lignin degradation. The TG curve shown in this work was comparable
358 to those found in literature for SBP (Li et al., 2014; Yilgin et al., 2010). Then, on the DTG
359 curve the peaks describe the maximum rate of weight loss occurred at different
360 temperatures (El-Sayed & Mostafa, 2014). First peak between 50 – 100 °C corresponded to
361 moisture drying. Then, having as a reference an study of separated pure hemicellulose,
362 pectin and cellulose pyrolysis (Fisher et al., 2002), the DTG peaks of the raw SBP were
363 identified by comparison to pure compounds curves. So that, the first peak of raw material
364 DTG shown at 258 °C was due to both pectin and hemicellulose degradation. Next peak at
365 304 °C was due to secondary pyrolysis of hemicellulose and the peak at 348 °C was
366 attributed to cellulose decomposition. That last peak was not only due to cellulose but also
367 to lignin (in a minor proportion).

368 On the other hand, when taking a look to the TG curve of the solid product after reaction a
369 similar behavior was found, with the cellulose, hemicellulose and pectins degradation curve
370 from 200 to 370 °C again. Then, instead of a continuous decreasing curve, two different
371 slopes were found, first one between 370 to 510 °C and second one between 510 and 740
372 °C. DTG curve was also analyzed and compared to previous studies. Both TG and DTG
373 curves obtained from the remaining solid in this work were comparable to those obtained
374 for dealkaline lignin from a previous work (Zhou et al., 2013). That dealkaline lignin from
375 that previous work showed two main peaks at the DTG curve, at around 350 and 750 °C.
376 That peaks were found for the solid product in this work, corroborating the lignin-like
377 nature of the solid obtained after FASTSUGARS process. Once the lignin nature of the
378 solid was confirmed, further explanation for the 500 °C peak was needed, as it was not
379 observed for other lignin DTG curves in previous works (Idris et al., 2010; Mohamad
380 Ibrahim et al., 2011; Zhou et al., 2013). For sugarcane bagasse it was found that this region
381 was related to the end of cellulose decomposition and the formation of char (El-Sayed &
382 Mostafa, 2014). So that, it seemed that char was produced during the FASTSUGARS
383 process, probably related to the transformation suffered by both cellulose and hemicellulose
384 trapped inside the cell wall network that could yield to the production of recalcitrant
385 humins from both 5-HMF and furfural (Sanchez-Bastardo & Alonso, 2017). It could be
386 concluded that the most recalcitrant fraction of the solid product, meaning acid-insoluble
387 fraction, was composed of insoluble lignin and char produced during the SCW hydrolysis.

388 To analyze the thermal behavior, several parameters were calculated through TGA results
389 and shown in Table 3 according to previous works (Cotana et al., 2014; Mohamad Ibrahim
390 et al., 2011). In first place, the temperature that produced 50 % degradation of the sample
391 was calculated. It can be seen that this temperature was higher for the treated solid, so it
392 could be said that after FASTSUGARS process, the resistance of the solid to thermal
393 degradation and therefore thermal stability was improved (shifting from 335 °C for the raw
394 SBP to 444 °C for the treated solid). The temperature to 50 % weight loss for the solid after
395 reaction (444 °C) was higher to the one found for kraft lignin (430 °C) (Mohamad Ibrahim
396 et al., 2011), corroborating again the lignin-like nature of the solid obtained after
397 FASTSUGARS process. Then, another way to show the thermal stability of the samples
398 was regarding the degradation produced between 200 – 600 °C. Within this range, all the
399 hydrolysable fractions were degraded and just lignin, char and ash remained. The raw SBP,
400 as it was mainly composed of those hydrolysable fractions, it suffered an important
401 degradation within that temperature range. On the contrary, as the solid after reaction was
402 mainly composed of an AIF comparable to insoluble lignin, it could better resist thermal
403 degradation within that range. The degradation value for the solid after FASTSUGARS
404 process (56 %) was consistent with values reported for other lignins (Sahoo et al., 2011). In
405 terms of ash content, it could be seen that ash content was around 8 times higher for the
406 solid after reaction compared to the raw material. After the FASTSUGARS process, the
407 hydrolysable fractions were removed from the remaining solid to the liquid product and
408 therefore the solid was concentrated in other compounds such as ash (see Fig. 3).

409 Then, FTIR analysis was performed to the raw material and the solid product obtained after
410 reaction (same conditions before: 390 °C, 25 MPa and 0.14 s) to have some insight about
411 the changes produced by the FASTSUGARS process in the chemical structure of the solid.
412 Both FTIR spectra were shown in Fig. S3 and, in order to compare, several regions were
413 identified and collected in Table S6. When comparing both spectra in Fig. S3, a remarkable
414 difference in the regions related to lignin was observed, since sharper peaks appeared for
415 the solid after reaction compared to the raw SBP (see detailed areas plotted in Fig. S3a,
416 S3b, S3c, S3d and S3e). So that, the enhancement of these peaks meant that the aromatic
417 nature of the solid after FASTSUGARS process was enhanced in detriment of its
418 carbohydrate content. In fact, the reduced carbohydrate content was obvious when

419 comparing the intensity of certain bands in the miscellaneous regions of the raw material
420 spectra (meaning regions related to cellulose, hemicellulose and lignin), so that when
421 removing the polysaccharides from the solid during the FASTSUGARS process, these
422 peaks were considerably reduced.

423 Through several analyses (acid hydrolysis, TGA and FTIR) it was proved that the solid
424 product obtained after FASTSUGARS process was mainly composed of an acid-insoluble
425 fraction (AIF), being a combination of insoluble lignin from the raw material and char
426 produced during SCW hydrolysis. Increasing the reaction time, the AIF increased in the
427 solid since the cellulose and hemicellulose were hydrolyzed until hollowing out the cell
428 wall leaving behind the most recalcitrant fractions of biomass: ash and acid-insoluble
429 residue. It was also proved that the FASTSUGARS treatment improved the thermal
430 properties of the solid and enhanced its aromatic nature.

431 As a step towards integrated biorefineries, coupling the SCW hydrolysis of SBP in the
432 exiting industrial facilities for sugar production would allow the energetic integration of the
433 process with current heat and power generation systems, like the gas turbine processes. So,
434 after sugar production from beet a wet by-product, meaning SBP, would be produced. If
435 that SBP would be directly feed to the FASTSUGARS process, three products would be
436 obtained: (1) a liquid product containing sugars and building blocks such as
437 glycolaldehyde; (2) a solid product with enhanced thermal properties and aromaticity and
438 (3) a high-pressure steam composed almost exclusively of water. Then, both liquid and
439 solid product should undergo downstream processes to obtain marketable products such as
440 ethylene glycol or sorbitol from the liquid and on the other hand, the solid fraction could be
441 purified to produce composite additives. Additionally, the steam could be injected to the
442 combustor of a gas turbine in order to increase the energy (shaft work) production (please
443 refer to previous work for concept evaluation (Cantero et al., 2015c)). Therefore, the
444 integration of the FASTSUGARS process would transform the sugar production process
445 into a closed loop system, increasing the value of the ending products (SBP mostly used as
446 animal feed would be converted to valuable building blocks) and reducing the energy
447 demand through the energetic integration developed in a previous work (Cantero et al.,
448 2015c).

481 Brunner, G. 2014. Chapter 8 - Processing of Biomass with Hydrothermal and Supercritical
482 Water. in: *Supercritical Fluid Science and Technology*, (Ed.) B. Gerd, Vol. Volume
483 5, Elsevier, pp. 395-509.

484 Cantero, D.A., Dolores Bermejo, M., José Cocero, M. 2013. High glucose selectivity in
485 pressurized water hydrolysis of cellulose using ultra-fast reactors. *Bioresource
486 Technology*, **135**, 697-703.

487 Cantero, D.A., Dolores Bermejo, M., José Cocero, M. 2015a. Reaction engineering for
488 process intensification of supercritical water biomass refining. *The Journal of
489 Supercritical Fluids*, **96**, 21-35.

490 Cantero, D.A., Martínez, C., Bermejo, M.D., Cocero, M.J. 2015b. Simultaneous and
491 selective recovery of cellulose and hemicellulose fractions from wheat bran by
492 supercritical water hydrolysis. *Green Chem.*, **17**(1), 610-618.

493 Cantero, D.A., Vaquerizo, L., Mato, F., Bermejo, M.D., Cocero, M.J. 2015c. Energetic
494 approach of biomass hydrolysis in supercritical water. *Bioresour Technol*, **179**, 136-
495 143.

496 Cocero, M.J., Cabeza, Á., Abad, N., Adamovic, T., Vaquerizo, L., Martínez, C.M., Pazo-
497 Cepeda, M.V. 2017. Understanding biomass fractionation in subcritical &
498 supercritical water. *The Journal of Supercritical Fluids*.

499 Concha Olmos, J., Zúñiga Hansen, M.E. 2012. Enzymatic depolymerization of sugar beet
500 pulp: Production and characterization of pectin and pectic-oligosaccharides as a
501 potential source for functional carbohydrates. *Chemical Engineering Journal*, **192**,
502 29-36.

503 Cotana, F., Cavalaglio, G., Nicolini, A., Gelosia, M., Coccia, V., Petrozzi, A., Brinchi, L.
504 2014. Lignin as Co-product of Second Generation Bioethanol Production from
505 Ligno-cellulosic Biomass. *Energy Procedia*, **45**, 52-60.

506 Chen, H.-m., Fu, X., Luo, Z.-g. 2016. Effect of molecular structure on emulsifying
507 properties of sugar beet pulp pectin. *Food Hydrocolloids*, **54**, 99-106.

508 Dasari, R.K., Eric Berson, R. The effect of particle size on hydrolysis reaction rates and
509 rheological properties in cellulosic slurries. (1559-0291 (Electronic)).

510 El-Sayed, S.A., Mostafa, M.E. 2014. Pyrolysis characteristics and kinetic parameters
511 determination of biomass fuel powders by differential thermal gravimetric analysis
512 (TGA/DTG). *Energy Conversion and Management*, **85**, 165-172.

513 Esposito, D., Antonietti, M. 2015. Redefining biorefinery: the search for unconventional
514 building blocks for materials. *Chem Soc Rev*, **44**(16), 5821-35.

515 Fisher, T., Hajaligol, M., Waymack, B., Kellogg, D. 2002. Pyrolysis behavior and kinetics
516 of biomass derived materials. *Journal of Analytical and Applied Pyrolysis*, **62**(2),
517 331-349.

518 Fukushima, R.S., Hatfield, R.D. 2004. Comparison of the Acetyl Bromide
519 Spectrophotometric Method with Other Analytical Lignin Methods for Determining
520 Lignin Concentration in Forage Samples. *Journal of Agricultural and Food
521 Chemistry*, **52**(12), 3713-3720.

522 Hansen, K.M., Thuesen, A.B., Sørensen, J.R. 2001. Enzyme assay for identification of
523 pectin and pectin derivatives, based on recombinant pectate lyase. *Journal of AOAC
524 International*, **84**(6), 1851-1854.

525 Himmel, M.E., Ding, S.-Y., Johnson, D.K., Adney, W.S., Nimlos, M.R., Brady, J.W.,
526 Foust, T.D. 2007. Biomass Recalcitrance: Engineering Plants and Enzymes for
527 Biofuels Production. *Science*, **315**(5813), 804-807.

- 528 Idris, S.S., Abd Rahman, N., Ismail, K., Alias, A.B., Abd Rashid, Z., Aris, M.J. 2010.
529 Investigation on thermochemical behaviour of low rank Malaysian coal, oil palm
530 biomass and their blends during pyrolysis via thermogravimetric analysis (TGA).
531 *Bioresour Technol*, **101**(12), 4584-92.
- 532 Jeong, H., Park, Y.C., Seong, Y.J., Lee, S.M. 2017. Sugar and ethanol production from
533 woody biomass via supercritical water hydrolysis in a continuous pilot-scale system
534 using acid catalyst. *Bioresour Technol*, **245**(Pt A), 351-357.
- 535 Kühnel, S., Schols, H.A., Gruppen, H. 2011. Aiming for the complete utilization of sugar-
536 beet pulp: Examination of the effects of mild acid and hydrothermal pretreatment
537 followed by enzymatic digestion. *Biotechnology for Biofuels*, **4**(1), 1-14.
- 538 Kumar, S., Gupta, R., Lee, Y.Y., Gupta, R.B. 2010. Cellulose pretreatment in subcritical
539 water: effect of temperature on molecular structure and enzymatic reactivity.
540 *Bioresour Technol*, **101**(4), 1337-47.
- 541 Leijdekkers, A.G., Bink, J.P., Geutjes, S., Schols, H.A., Gruppen, H. 2013. Enzymatic
542 saccharification of sugar beet pulp for the production of galacturonic acid and
543 arabinose; a study on the impact of the formation of recalcitrant oligosaccharides.
544 *Bioresour Technol*, **128**, 518-25.
- 545 Li, M., Wang, L.J., Li, D., Cheng, Y.L., Adhikari, B. 2014. Preparation and
546 characterization of cellulose nanofibers from de-pectinated sugar beet pulp.
547 *Carbohydr Polym*, **102**, 136-43.
- 548 Lynch, M.B., O'Shea, C.J., Sweeney, T., Callan, J.J., O'Doherty, J.V. 2008. Effect of crude
549 protein concentration and sugar-beet pulp on nutrient digestibility, nitrogen
550 excretion, intestinal fermentation and manure ammonia and odour emissions from
551 finisher pigs. *Animal*, **2**(3), 425-34.
- 552 Martínez, C.M., Cantero, D.A., Bermejo, M.D., Cocero, M.J. 2015. Hydrolysis of cellulose
553 in supercritical water: reagent concentration as a selectivity factor. *Cellulose*, **22**(4),
554 2231-2243.
- 555 Merino, S.T., Cherry, J. 2007. Progress and Challenges in Enzyme Development for
556 Biomass Utilization. in: *Biofuels*, (Ed.) L. Olsson, Springer Berlin Heidelberg.
557 Berlin, Heidelberg, pp. 95-120.
- 558 Mohamad Ibrahim, M.N., Zakaria, N., Sipaut, C.S., Sulaiman, O., Hashim, R. 2011.
559 Chemical and thermal properties of lignins from oil palm biomass as a substitute for
560 phenol in a phenol formaldehyde resin production. *Carbohydrate Polymers*, **86**(1),
561 112-119.
- 562 Okajima, I., Sako, T. 2014. Energy conversion of biomass with supercritical and subcritical
563 water using large-scale plants. *Journal of Bioscience and Bioengineering*, **117**(1), 1-
564 9.
- 565 Peterson, A.A., Vogel, F., Lachance, R.P., Froling, M., Antal, J.M.J., Tester, J.W. 2008.
566 Thermochemical biofuel production in hydrothermal media: A review of sub- and
567 supercritical water technologies. *Energy & Environmental Science*, **1**(1), 32-65.
- 568 Prado, J.M., Lachos-Perez, D., Forster-Carneiro, T., Rostagno, M.A. 2016. Sub- and
569 supercritical water hydrolysis of agricultural and food industry residues for the
570 production of fermentable sugars: A review. *Food and Bioproducts Processing*, **98**,
571 95-123.
- 572 Romero, A., Cantero, D., Nieto-Marquez, A., Martinez, C., Alonso, E., Cocero, M.J. 2016.
573 Supercritical water hydrolysis of cellulosic biomass as effective pretreatment to

574 catalytic production of hexitols and ethylene glycol over Ru/MCM-48. *Green*
575 *Chemistry*.

576 Sahoo, S., Seydibeyoğlu, M.Ö., Mohanty, A.K., Misra, M. 2011. Characterization of
577 industrial lignins for their utilization in future value added applications. *Biomass*
578 *and Bioenergy*, **35**(10), 4230-4237.

579 Sanchez-Bastardo, N., Alonso, E. 2017. Maximization of monomeric C5 sugars from wheat
580 bran by using mesoporous ordered silica catalysts. *Bioresour Technol*, **238**, 379-
581 388.

582 Saulnier, L., Thibault, J.-F. 1999. Ferulic acid and diferulic acids as components of sugar-
583 beet pectins and maize bran heteroxylans. *Journal of the Science of Food and*
584 *Agriculture*, **79**(3), 396-402.

585 Sluiter, J.B., Ruiz, R.O., Scarlata, C.J., Sluiter, A.D., Templeton, D.W. 2010.
586 Compositional Analysis of Lignocellulosic Feedstocks. 1. Review and Description
587 of Methods. *J. Agric. Food Chem.*, **58**(16), 9043-9053.

588 Spagnuolo, M., Crecchio, C., Pizzigallo Maria, D.R., Ruggiero, P. 2000. Fractionation of
589 sugar beet pulp into pectin, cellulose, and arabinose by arabinases combined with
590 ultrafiltration. *Biotechnology and Bioengineering*, **64**(6), 685-691.

591 Vaquerizo, L., Cocero, M.J. 2018. A green desuperheater for an energetic efficient
592 alternative to the decompression valve in biomass supercritical water ultrafast
593 hydrolysis process. *The Journal of Supercritical Fluids*, **133**, 704-715.

594 Wahyudiono, Sasaki, M., Goto, M. 2008. Recovery of phenolic compounds through the
595 decomposition of lignin in near and supercritical water. *Chemical Engineering and*
596 *Processing: Process Intensification*, **47**(9-10), 1609-1619.

597 Yılgin, M., Deveci Duranay, N., Pehlivan, D. 2010. Co-pyrolysis of lignite and sugar beet
598 pulp. *Energy Conversion and Management*, **51**(5), 1060-1064.

599 Zhao, Y., Lu, W.J., Wu, H.Y., Liu, J.W., Wang, H.T. 2012. Optimization of supercritical
600 phase and combined supercritical/subcritical conversion of lignocellulose for hexose
601 production by using a flow reaction system. *Bioresour Technol*, **126**, 391-6.

602 Zheng, Y., Lee, C., Yu, C., Cheng, Y.-S., Zhang, R., Jenkins, B.M., VanderGheynst, J.S.
603 2013. Dilute acid pretreatment and fermentation of sugar beet pulp to ethanol.
604 *Applied Energy*, **105**, 1-7.

605 Zhou, H., Long, Y., Meng, A., Li, Q., Zhang, Y. 2013. The pyrolysis simulation of five
606 biomass species by hemi-cellulose, cellulose and lignin based on thermogravimetric
607 curves. *Thermochimica Acta*, **566**, 36-43.

608 Zieminski, K., Romanowska, I., Kowalska-Wentel, M., Cyran, M. 2014. Effects of
609 hydrothermal pretreatment of sugar beet pulp for methane production. *Bioresour*
610 *Technol*, **166**, 187-93.

611

612

613 **Tables and Figures captions**

614 Table 1. Compositional analysis for SBP (dry basis).

615 Table 2. Input data for SBP hydrolysis calculations in SCW in the FASTSUGARS plant.

616 Five samples per experiment were collected to be representative.

617 Table 3. Thermal properties for raw SBP and solid collected after SCW hydrolysis at

618 FASTSUGARS process (392 °C, 25 MPa, 0.14s).

619 Figure 1. Yields of main compounds after SCW hydrolysis of SBP at 390°C and 25MPa in

620 the FASTSUGARS plant at different reaction times. The sum of glycolaldehyde,

621 pyruvaldehyde and glyceraldehyde were labeled as ‘RAC’ and lactic, formic, acetic and

622 galacturonic acids were named as ‘ACIDS’.

623 Figure 2. Schematic reaction pathway for cellulose, hemicellulose and pectin in biomass

624 under SCW hydrolysis conditions.

625 Figure 3. Composition of the solid product obtained after SCW hydrolysis of SBP at 390°C

626 and 25 MPa in the FASTSUGARS plant at different reaction times, compared to raw

627 material. AIF = acid-insoluble fraction, SL = soluble lignin, SUGARS = sugars from

628 hydrolyzed cellulose, hemicellulose and pectin. See Table S5 for detailed solid

629 composition.

630 Figure 4. TG and DTG curves for the raw SBP and the solid obtained after SCW hydrolysis

631 in the FASTSUGARS process at 3920°C, 25 MPa and 0.14 s. (P =pectin degradation; H =

632 hemicellulose degradation; C = cellulose degradation; L = lignin degradation).

633

634

635

636

637

638

639 **Tables**

640 **Table 1.**

Lignin	Ash	Cellulose	Hemicellulose	Proteins	Pectins	Extractives
23.9%	1.3%	16.6%	19.7%	9.5%	27.5%	1.9%

641

642

643

644 **Table 2.**

EXP	t_R (s)	T (°C)	P (bar)	ρ_r (kg/m ³)	C_{in} (% w/w)	suspended solids (% w/w)	TOC (ppmC)
1	0.11	392	250	199	1.90	0.15	5883
2	0.14	392	251	213	1.68	0.13	5093
3	0.19	395	249	179	1.64	0.06	5189
4	0.23	393	256	221	1.72	0.12	5092
5	1.15	393	251	198	1.73	0.03	5386

645

646

647

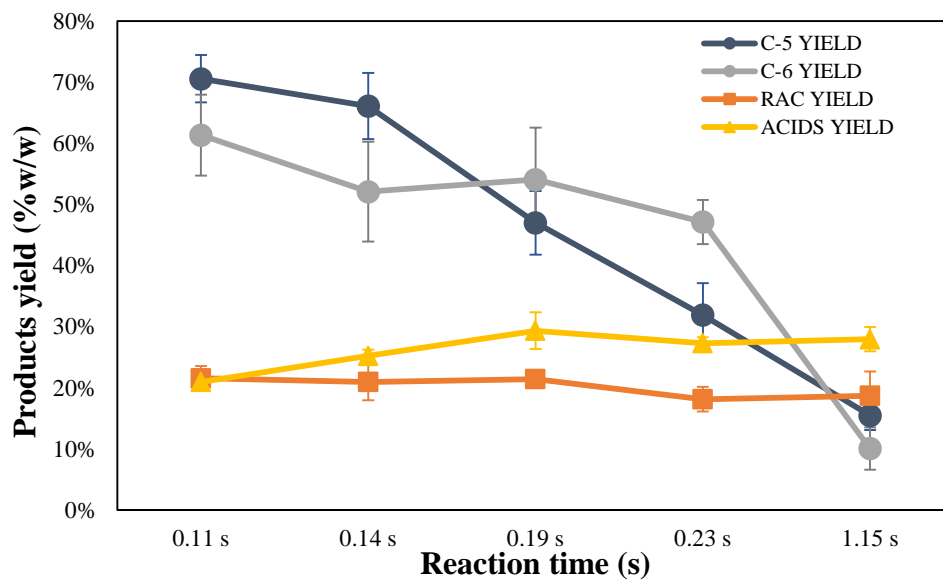
648 **Table 3.**

649

	Raw SBP	After reaction
Temperature at 50% degradation (°C)	335	444
Degradation between 200 – 600 (% w/w)	74.59	55.47
Ash (% w/w)	2.23	16.81

650 **Figures**

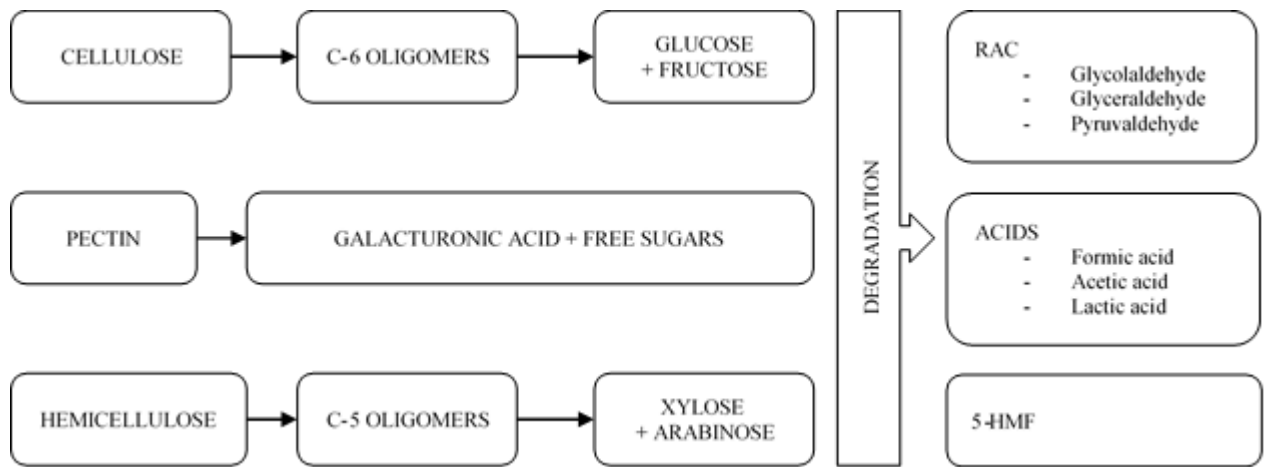
651 **Figure 1.**



652

653

654 **Figure 2.**



655

656

657

658

659

660

661

662

663

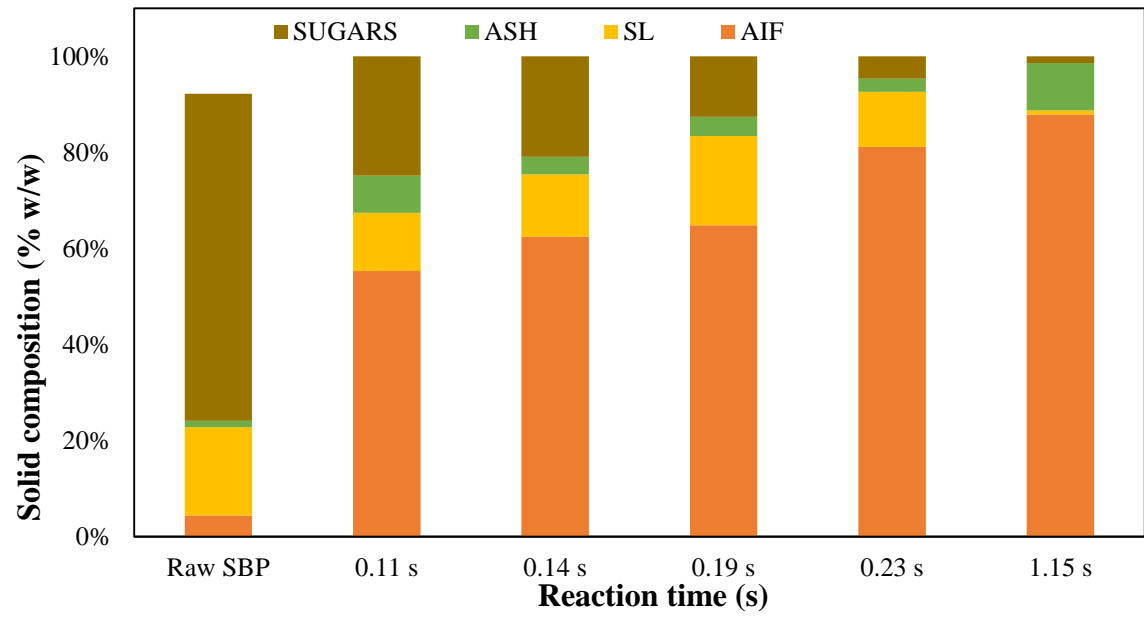
664

665

666

667 **Figure 3.**

668

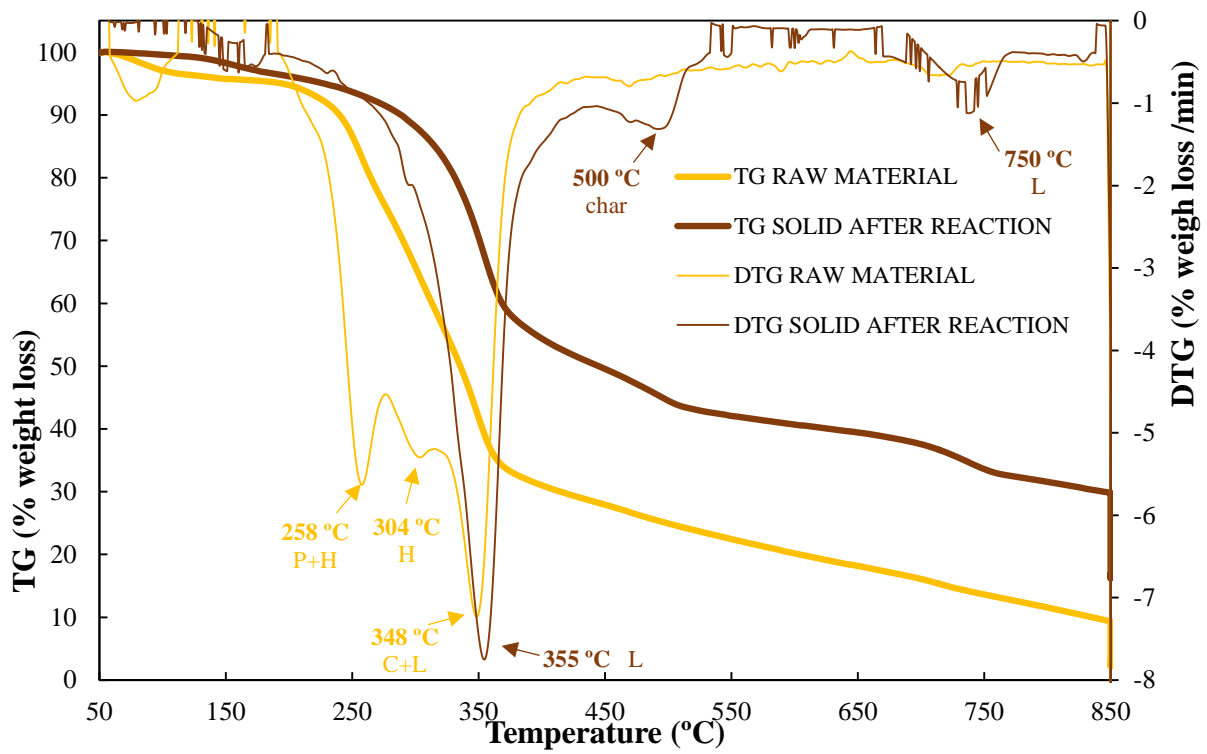


669

670

671 **Figure 4.**

672



673
674

675

676